67. Diffuse Hepatic Pathology

The versatility of MRI enables comprehensive evaluation of diffuse liver disease. Figure 67.1A-C illustrates findings characteristic of a fatty liver on FSE T2, in-phase, and out-of-phase GRE T1WI, respectively. Within the lateral right liver lobe an area of subtly decreased SI can be differentiated from the relatively high signal intensity surrounding liver parenchyma on (A) T2WI representing focal fatty sparing. On (B) in-phase T1WI, the liver appears hyperintense due to diffuse fatty infiltration, although this is difficult to assess without comparison to the spleen. (C) Out-of-phase images clearly demonstrate signal loss diffusely within the liver with the exception of the spared focus. This SI loss results from negation of opposed water and fat signals as described more in detail in Chapter 69. Fat suppression (FS) imaging detects mild fatty infiltration less sensitively than in- and out-of-phase imaging, as SI suppression from fat saturation when a small amount of fat is present is approximately half of that obtained in out-of-phase images which suppress both fat SI and that of water (when present in the same voxel), the latter from destructive signal interference. Fat-predominant lesions are better detected with FS imaging. The T2WI of Fig. 67.1D demonstrate a relatively hypointense lesion (white arrow) in a liver diffusely infiltrated by fat, as evident on (E) in and (F) out-of-phase images. The typical location adjacent to the gallbladder fossa and the lack of abnormal enhancement on (G) in-phase CE T1WI implies an area of focal fatty sparing and excludes a malignant focal liver lesion (which would typically show no signal dropout on out-of-phase images either).

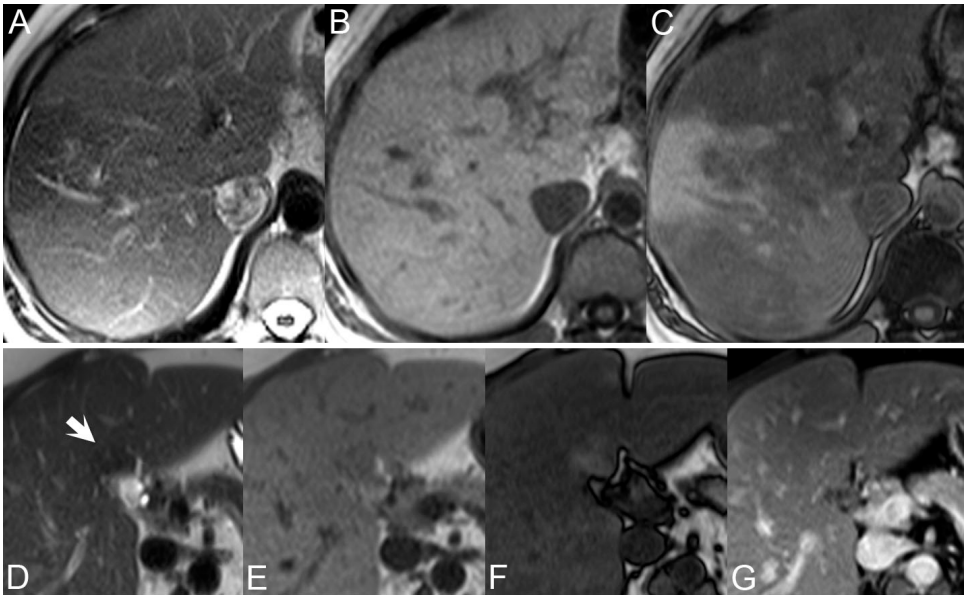

Fig. 67.1

Post-contrast out-of-phase imaging results in a paradoxical loss in fatty tissue SI: tissues consisting of mainly fat still contain some amount of water, the SI contribution from which is disproportionately small due to the long T1 of water. Gadolinium chelates shorten the T1 time of water in the extracellular space, resulting in a greater contribution of water protons to SI. With out-of-phase images, this results in more destructive interference with fat, decreasing SI.

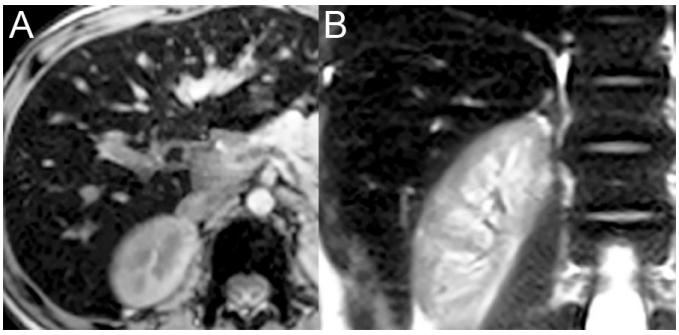

Fig. 67.2

Accumulation of intracellular paramagnetic iron products—in distinction to copper (as in Wilson's disease)—results in magnetic field inhomogeneities that increase T2* decay and lead to a low SI on GRE T2WI. The patient in Fig. 67.2 had received multiple blood transfusions, resulting in secondary hemochromatosis with reticuloendothelial iron content leading to diminished SI on (A) axial and (B) coronal HASTE T2WI within both the liver and bone marrow. Iron deposition in the reticuloendothelial system in secondary hemochromatosis and hemosiderosis does not directly damage parenchymal cells and spares the pancreas, progressively affecting the liver, spleen, and myocardium. Parenchymal iron deposition occurs directly in primary hemochromatosis, affecting the liver, pancreas, and myocardium but not the spleen. A dysfunctional or saturated reticuloendothelial system in secondary hemochromatosis may blur the latter point of distinction. Iron deposition and resulting hepatocellular damage predisposes to the development of hepatocellular carcinoma. The resulting hypointensity in the liver on T2* and T2WI provides natural contrast—similar in principle to that obtainable with superparamagnetic iron oxide (SPIO) contrast agents—to aid in the detection of hepatocellular carcinoma, which is depicted with higher SI than surrounding liver tissue. The earliest findings of liver cirrhosis include medial segment atrophy and hilar enlargement with fatty infiltration. Atrophy of the entire right lobe occurs later with left lateral and caudate lobe hypertrophy, the later more prominent in alcohol-induced cirrhosis. Other morphologic changes include right posterior segment notching and gallbladder fossa enlargement with fatty infiltration. Focal or diffuse fibrotic changes may occur, the former

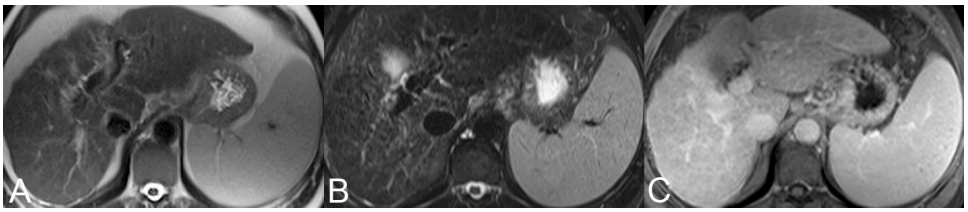

Fig. 67.3

illustrated in Fig. 67.3 where a focus of fibrosis is hyperintense to parenchyma on (A) HASTE T2 and (B) STIR T2WI. (C) In distinction to HCC, focal or diffuse liver fibrosis do not present with arterial hypervascularization and suspicious washout but rather show a homogeneous subtle enhancement on equilibrium phase CE T1WI. Liver contour in Fig. 67.3 is typically nodular (as seen in cirrhotic liver).

Splenomegaly—present in Fig. 67.3—typifies portal hypertension, as does the presence of varices at porto-systemic anastomoses, the latter appearing as dilated venous vessels with prominent flow-voids on T2WI. Portal venous flow may be assessed via MRA, with venous anatomy well-depicted on 2D TOF imaging and flow direction confirmed on phase contrast studies. CE MRA is especially useful if portal vein thrombosis, which appears as a filling defect, is suspected or if stagnant flow impairs 2D TOF. Areas of avid parenchymal enhancement are seen in portal vein thrombosis due to the increased dependence of the parenchyma on systemic blood supply. The wedge shape of such lesions distinguishes them from the heterogeneous enhancement seen in congestive heart failure due to increased sinusoidal pressure delaying parenchymal arterial flow. Acute hepatitis may be detected as patchy enhancement on arterial phase post-contrast imaging.